NEG

Water dissociation and selective absorption in the $Zr[V_{0.5}Fe_{0.5}]_2$ gettering alloy: An x-ray photoemission spectroscopy investigation

E. Narducci and J. Kovac[a)]
Laboratorio Nazionale TASC-INFM, Padriciano 99, I-34012 Trieste, Italy

F. Ghezzi and N. Venkataramani
Istituto di Fisica del Plasma, Associazione EURATOM/ENEA/CNR, Milano, Italy

M. Sancrotti[b)]
Laboratorio Nazionale TASC-INFM, Padriciano 99, I-34012 Trieste, Italy and
Istituto di Fisica del Plasma, Associazione EURATOM/ENEA/CNR, Milano, Italy

(Received 2 February 1998; accepted 18 December 1998)

We report a study, based on x-ray photoemission spectroscopy, on the effects of element-specific selective absorption of the nonevaporable $[Zr(V_{0.5}Fe_{0.5})_2]$ gettering alloy after massive exposure to water vapor (3×10^3 Pa for ≈2000 h at 400 °C). The specimens have been analyzed both after scraping and along a prolonged Ar^+ sputtering in order to comparatively discriminate intergranular *versus* intragranular properties. Oxygen is found to diffuse into the bulk of the alloy grains giving a distribution of Zr oxides where ZrO_2 is the major component. After removal of the outermost atomic layers, Fe and V show a major metallic character in the alloy volume. Traces of Zr hydroxides are also seen. The virgin (nonwater treated) $[Zr(V_{0.5}Fe_{0.5})_2]$ alloy has also been comparatively measured. © *1999 American Vacuum Society.* [S0734-2101(99)05402-0]

I. INTRODUCTION

Nonevaporable gettering alloys are well established tools in vacuum research and industry, their applications encompassing gas purification, hydrogen storage, attainment of ultrahigh vacuum (UHV), molecule dissociation, etc.[1–5] While extensive studies have focused macroscopic properties of these alloy systems such as pumping speed and capacity, fewer studies have been dedicated to monitor how the surface and near-surface properties of these alloys evolve at a microscopic scale as a function of different physical and chemical parameters such as temperature, gas exposure, and surface preparation.[5–11] A major point is to understand whether and to what extent macroscopic and microscopic properties are tuned to each other, this goal being of relevance both for near-surface and bulk behavior. Based on the evolution of other domains of material science, it is believed that a thorough evaluation of nonevaporable gettering alloys (NEG) could positively dictate effective engineering of novel custom-designed getters responding to the progressively increasing demand for more sophisticated properties.[12]

A specific area of great strategic importance deals with the ability of recycling tritiated water circulating in thermonuclear fusion reactors. In this context, recent studies have established that the NEG $[Zr(V_{0.5}Fe_{0.5})_2]$ alloy can efficiently dissociate water vapors with high doses of oxygen and hydrogen being retained and released, respectively.[13–15] Important aspects of the macroscopic behavior of this NEG alloy have been studied as a function of various parameters such as conversion temperature and pressure. However, a thorough description of the microchemistry occurring inside the alloy after water molecule dissociation and conversion is still lacking.

In this article, we report a systematic study based on a multitechnique approach of the $[Zr(V_{0.5}Fe_{0.5})_2]$ alloy both in the virgin version and after water conversion. The alloys were in the form of compressed pills of grain powders whose grains could contain a high number (>30) of single-crystal grains. X-ray photoemission spectroscopy (XPS) has been utilized for monitoring the elemental distribution and the chemical environment local to the various atomic sites in the near-surface region and also in the bulk. The bulk properties of this alloy have been characterized combining XPS with two distinct *in situ* preparation protocols: ion sputtering and mechanical scraping. This allows one to discriminate between the intragrain behavior (sputtering) and the intergrain state (scraping) since the former method removes atomic layers from the surfaces of the powder grains while the latter exposes primarily surfaces of the powder grains.

II. EXPERIMENT

$[Zr(V_{0.5}Fe_{0.5})_2]$ shows a C14 hexagonal crystallographic structure (lattice spacings: $a=5.05$ Å; $c=8.30$ Å). Ingots of $[Zr(V_{0.5}Fe_{0.5})_2]$ have been ground (typical grain size ≈10 μm) and the resulting powders have been compressed, at room temperature, obtaining cylindrical pills of about 10 mm height and 10 mm diameter. The virgin pills did not undergo any other processing. The water-treated (WT) specimens have been treated in a properly designed reactor described elsewhere.[13–15] The pills were exposed to water vapor at a pressure of 3×10^3 Pa for ≈2000 h of conversion with the sample temperature at 400 °C.

The XPS measurements were performed *ex situ* in a ul-

a)Present address: Institute of Surface Engineering and Optoelectronics, Teslova 30, 1000 Ljubljana, Slovenia.
b)Also at: Dipartimento di Fisica, Politecnico di Milano, Milano Italy: Electronic mail: sancrotti@sci.area.trieste.it

trahigh vacuum (base pressure $\approx 1\times10^{-10}$ mbar) apparatus. A nonmonochromatized Mg-anode source ($h\nu = 1253.6$ eV) was used for exciting photoelectrons which were analyzed in energy using a double-pass cylindrical mirror analyzer (CMA) operated in the retarding mode (energy resolution $\approx$0.3 eV). A differentially pumped Ar^+-ion gun (primary energy $\approx$3 keV) at grazing incidence was used for sputtering. The area rastered by the ion beam was set to be larger than the area sampled by the CMA. Therefore, the XPS spectra correspond to the deepest part of the sputtering-induced crater. During depth-profiling spectra acquisition was alternated with sputtering. Scraping of the samples was performed by means of diamond files.

Fitting of the Zr 3*d* core level line shapes was performed in terms of Voigt functions whose basic Gaussian and Lorentzian components were appropriately chosen in accordance with instrumental resolution [full-width at half-maximum (FWHM) $\approx$1.0 eV] and literature data concerning core hole lifetime broadening ($\approx$0.1 eV). The spin-orbit splitting of the Zr 3*d* emission was set equal to 2.4 eV with a branching ratio $\approx$1.5, in agreement with the literature. We note that the Gaussian width introduced in the fit analysis was a little bit higher than that expected just from instrumental resolution. This is typical of these Zr-based alloys and correspond to an inhomogeneous distribution of the distinct atomic sites corresponding to a selected oxidation state. The fitting routine included also a Shirley background mimicking the structureless secondary emission.

III. RESULTS AND DISCUSSION

The temperature-dependent near-surface chemistry of ingots of $[Zr(V_{0.5}Fe_{0.5})_2]$ has been recently studied via XPS by some of the authors,[11] this yielding a useful reference point for the chemical evaluation of the ground pills.

Figure 1 shows a stack of Zr 3*d* core level XP spectra obtained while depth profiling one of the WT pills. The top curve should correspond to a depth of $\approx$0.7 μm with respect to the pristine surface, i.e., a depth comparable to the average size of the single-crystal grains of the powders. From a visual inspection, it is easily recognized that no drastic changes occur in the Zr 3*d* spectra. The line shape fit for one of these Zr 3*d* spectra, intermediate within the depth profile, is given in Fig. 2. The resulting components can be associated with a series of Zr-suboxides encompassing the Zr^{4+}, Zr^{3+}, and Zr^{2+} oxidation states.[5,7–11,16–18] A sizeable component appears at higher binding energies (BE) and is ascribed to Zr atoms coordinated to (OH) groups, a result consistent with literature data.[18] An additional weak doublet was included in the fit, most probably due to Zr atoms differently bonded to residuals of water molecules. An overall quantitative view of the depth profile is given in Fig. 3 where the relative intensities of the chemically distinct Zr 3*d* components (see Fig. 2) are plotted as a function of the sputtering time. Apart from the initial transient, where the oxidation of the surface is dominated by the exposure to air (with subsequent C-based contamination) Fig. 3 indicates that the chemical state local to the Zr sites is homogeneous over the entire sputtered depth. Homogeneity of the WT specimen is also seen in Fig. 4 where the relative atomic concentrations of the chemical elements observed by XPS are given as a function of sputtering time. Concentrations were determined from the core-level peak areas after normalization to atomic sensitivity factors.[16] Except for the very short initial transient, the various chemical species are distributed essentially uniformly from the surface region down to the actual bulk of the grains. Concerning the depth profile, we note that:

(1) A minor C component is always present in the spectra,

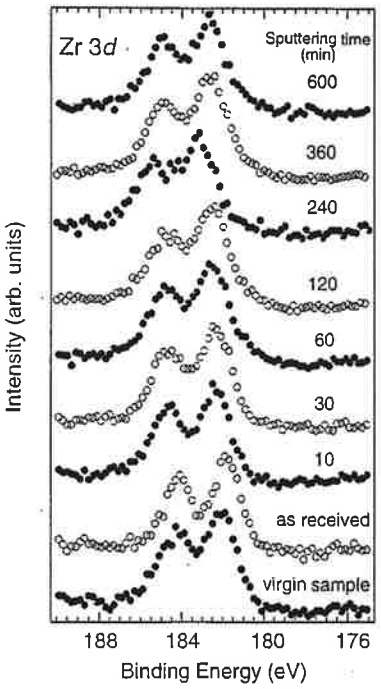

FIG. 1. Stack of Zr 3*d* core level XPS spectra as function of sputtering time for the WT sample. An XPS spectrum from an as-received nontreated (virgin) sample is also shown.

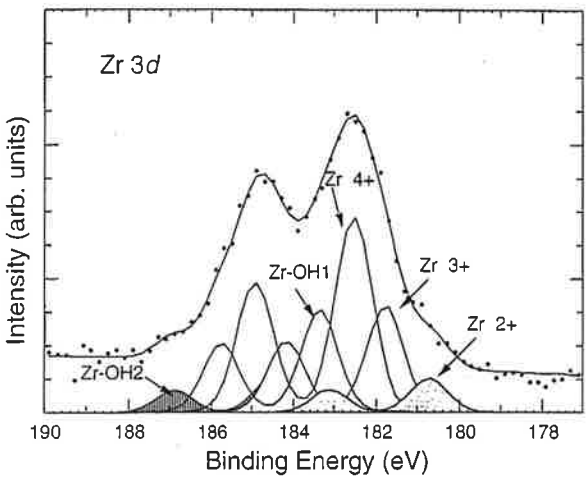

FIG. 2. Line shape analysis for the Zr 3*d* emission taken after 60 min of sputtering for the WT sample.

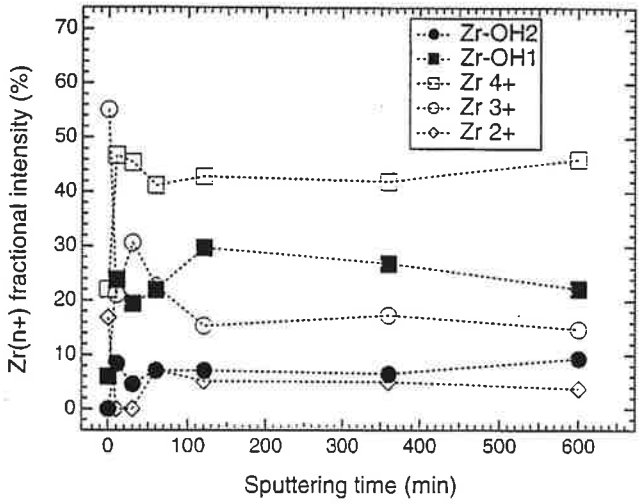

FIG. 3. Distribution of chemically distinct Zr $3d$ components as a function of the sputtering time. The data refer to the WT sample. Relative intensities are given in the profile.

this being probably due to shadowing effects associated with the sputtering beam and the irregular morphology of the pill surface.

(2) The relative concentrations of the metallic species Zr, V, Fe are not found in the stoichiometric ratio of the nominal pure alloy. In the literature,[19] the atomic sputtering yields of Zr, V, and Fe differ by factor of 2, for an Ar^+-ion beam of 3 keV energy. Vedel and Schlapbach[10] reported Zr enriched surfaces of $ZrV_{0.63}Fe_{0.13}$ due to preferential sputtering of V and Fe.

(3) Oxygen dominates by far with respect to all other elements, in spite of its lower atomic weight which should provide a higher sputtering yield. Stoichiometric ZrO_2 samples have been reported to be preferentially enriched of Zr when sputtered with the same conditions used in this article. Moreover, the sputtering process induces a reduction to lower oxidation states.[19] On this basis, we can conclude that the oxygen concentration reported in Fig. 4, which is around 60%, is lower than the real value. This is an unambiguous marker of the presence of oxygen well below the near-surface region.

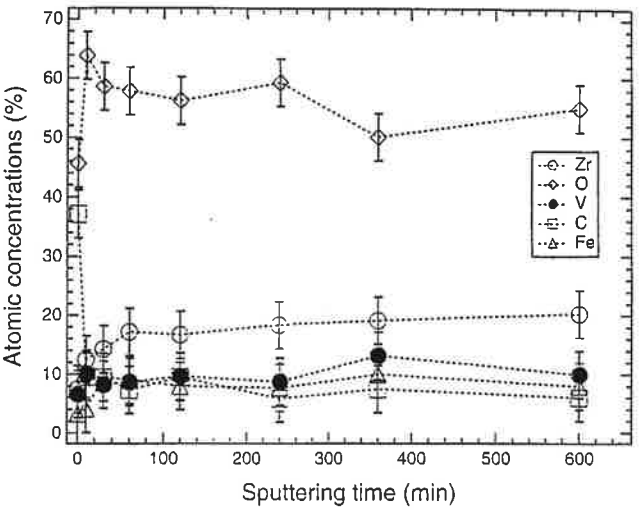

FIG. 4. The atomic concentrations depth profile of the WT sample.

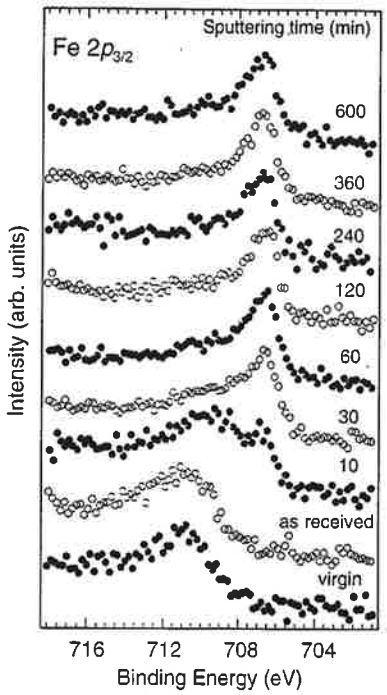

FIG. 5. Stack of Fe $2p_{3/2}$ core level XPS spectra as function of sputtering time for the WT sample. An XPS spectrum from an as-received nontreated (virgin) sample is also shown.

The depth profile of Fig. 4 points out unambiguously that the absorption of oxygen derived from water molecules is a bulk process and is limited neither to the pill surface nor to the surfaces of the single-crystal grains of alloy where oxidation processes could easily take place via diffusion along the grain boundaries. On the average, the ratio of the relative concentrations of Zr and O is very close to that of stoichiometric ZrO_2, which is consistent with the fit of the Zr $3d$ line shape (Fig. 2). In contrast to from the Zr $3d$ line shape, the Fe $2p$ core level XP spectra exhibit drastic changes in shape while depth profiling the WT specimen. This is seen in Fig. 5 where a stack of Fe $2p$ curves is shown at selected sputtering times. While the initial spectra are characterized by high oxidation states corresponding to a variety of Fe oxides (Fe_2O_3, Fe_3O_4, FeO), for sputtering times greater than about 30 (60) min the spectra are dominated by metal-like emission (BE≈706.5 eV) due to Fe atoms primarily coordinated to other metal atoms.[9–11,16]

The behavior of the V $2p$ core-level spectra is similar to the Fe $2p$ results of Fig. 5. A series of spectra for selected sputtering times is shown in Fig. 6. While the near-surface region of the WT specimen is typical of a mixture of V oxidized states, the layers underneath are characterized by metal-like V as demonstrated by the peaked emission at ≈512 eV.[5,8–10,16]

To better understand the effects of water dissociation and adsorption in the $[Zr(V_{0.5}Fe_{0.5})_2]$ alloy and distinguish these

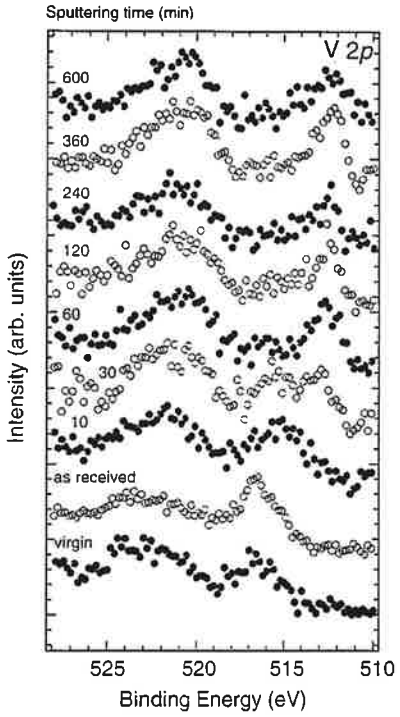

FIG. 6. Stack of V $2p$ core level XPS spectra as a function of sputtering time for the WT sample. An XPS spectrum from an as-received nontreated sample (virgin) is also shown.

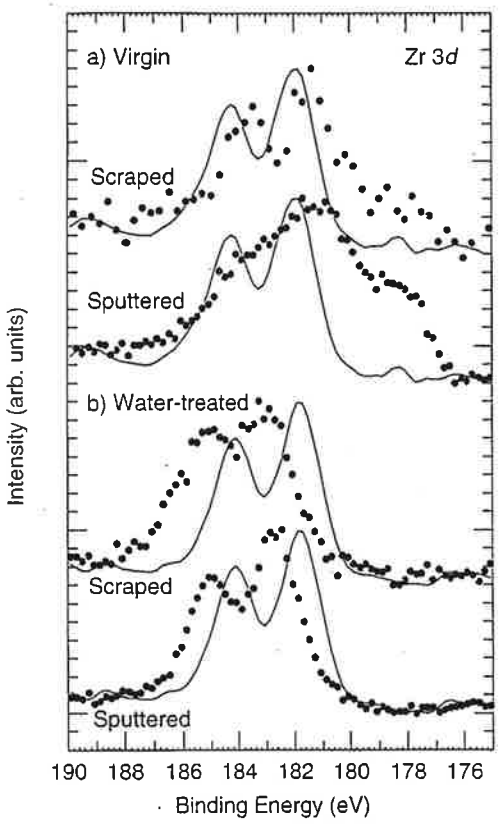

FIG. 7. Zr $3d$ spectra of WT and virgin $Zr[V_{0.5}Fe_{0.5}]_2$ samples after sputtering and scraping. The solid line is for the as-received specimens.

effects from ordinary oxidation due to air exposure, we now compare the results obtained from virgin pills of the $[Zr(V_{0.5}Fe_{0.5})_2]$ alloy. For both samples, spectra measured from as-received specimens and after sputtering or scraping will be jointly analyzed. The underlying basic idea is that the massive action of the scraping process should primarily expose grain boundaries of the powder grains (intergranular properties) while the softer ion-induced erosion should give a direct insight into the chemistry occurring inside the single-crystal grains, that is intragranular properties should be inferred.

This is shown in Figs. 7–10 for the Zr $3d$, Fe $2p$, V $2p$, and O $1s$ emissions. In these figures, the solid lines indicate data for the as-received specimens while the dots mark spectra taken after *in situ* treatment (ion-induced erosion or scraping).

Removal via sputtering of the topmost atomic layers of the virgin pills of the $[Zr(V_{0.5}Fe_{0.5})_2]$ alloy reveals Zr $3d$ metallic components characterized by lower BE ($Zr\,3d_{5/2} \approx 178.6$ eV) with respect to the suboxides. If the specimen is scraped, most of the Zr $3d$ signal is still associated with Zr oxides with just a weak intensity from the metal, this indicating that Zr is oxidized not only at the actual surface of the pills but also at the grain boundaries. In contrast, the WT $[Zr(V_{0.5}Fe_{0.5})_2]$ alloy shows an opposite trend. Spectra for both the intergranular and intragranular specimens show a sizeable shift of the spectral weight toward higher BEs which reflects a relative increase of the high oxidation states (primarily Zr^{4+}) and, remarkably, a non-negligible contribution due to Zr atoms coordinated to hydroxyl groups. This latter assignment clarifies an important point concerning the potential application of the alloy for recycling tritiated water. Actually, part of the (OH)-related groups diffuse into the bulk of the powder grains and this demonstrates at a microscopic level that not all the hydrogen is released by the $[Zr(V_{0.5}Fe_{0.5})_2]$ alloy after water molecule dissociation. We notice that formation of Zr hydrides can be excluded since $Zr\,3d_{5/2}$ from Zr hydrides would be expected around 179–179.6 eV BE.[20] Remarkably, the XPS findings on the WT specimen are in agreement with a model formulated on the basis of volumetric measurements.[21]

Sputtering of both the virgin and WT alloy yields a major metal-like component in the spectra of the Fe $2p$ (Fig. 8) and V $2p$ (Fig. 9) core line emissions with the parallel extinction of the spectral components related to oxides. A somehow different scenario emerges after scraping where the partial increase of the metal-like components at low BEs does not deplete all the oxide-related contributions (Figs. 8 and 9). This finding holds for both the virgin and WT specimens, the latter showing a more pronounced oxidation. The traces of Fe and V oxides still visible after scraping are again assigned to the mostly oxidized grain boundaries due to diffusion of contaminants along the grain boundaries.

Also significant is the outcome of the O $1s$ line shape analysis (Fig. 10). The as-received surface of both the specimens is characterized by two major components: one is centered at ≈530 eV BE and is typical of Zr oxides while the other at ≈532 eV corresponds to variously chemisorbed

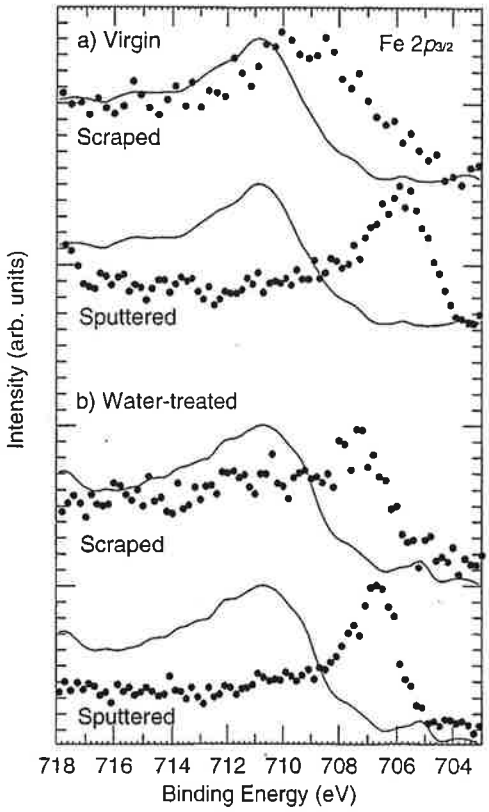

FIG. 8. Fe $2p_{3/2}$ spectra of WT and virgin $Zr[V_{0.5}Fe_{0.5}]_2$ samples after sputtering and scraping. The solid line is for the as-received specimens.

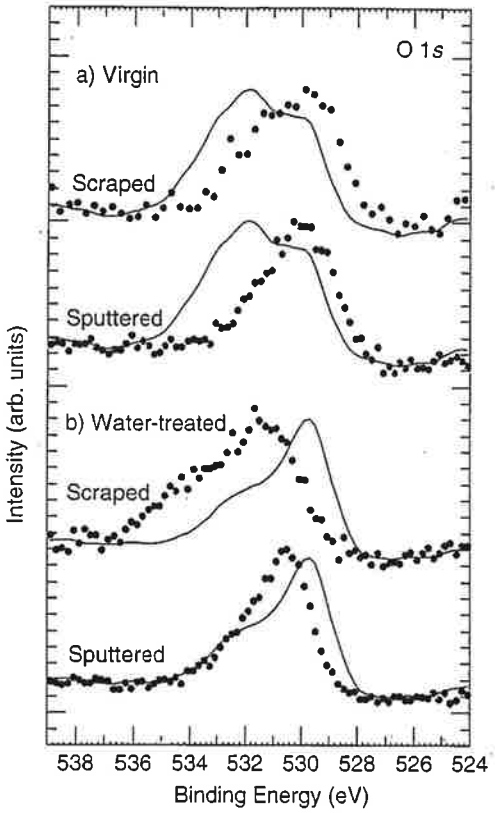

FIG. 10. O 1*s* spectra of WT and virgin $Zr[V_{0.5}Fe_{0.5}]_2$ samples after sputtering and scraping. The solid line is for the as-received specimens.

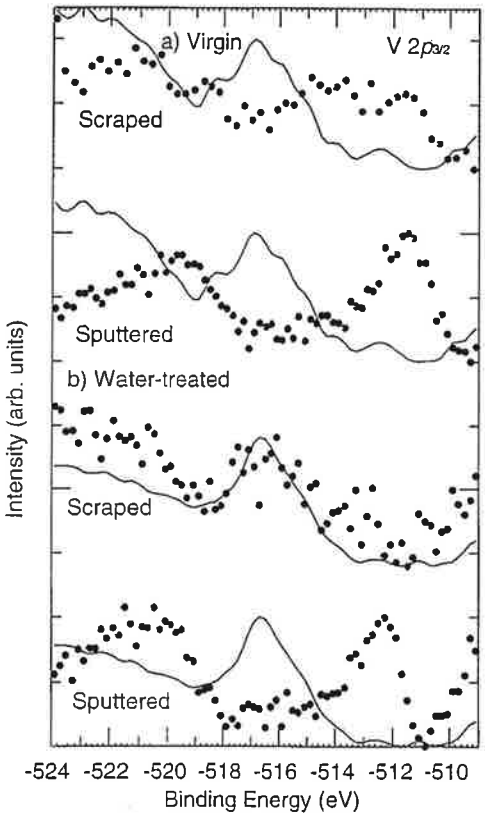

FIG. 9. V $2p$ spectra of WT and virgin $Zr[V_{0.5}Fe_{0.5}]_2$ samples after sputtering and scraping. The solid line is for the as-received specimens.

(OH) groups.[5,7–11,18] Both the *in situ* surface treatments of the virgin $[Zr(V_{0.5}Fe_{0.5})_2]$ alloy yield a spectral weight shifted to lower BE with respect to the as-received surface, this being consistent with stronger contributions to the O 1*s* line shape derived from Zr oxides[22] and a partial depletion of the spectral weight relative to (OH) groups. Interestingly, a clear shift toward higher BE is seen on the WT specimen after either ion-induced erosion or scraping. This is a clear indication of the existence of hydroxyl groups, mostly coordinated to Zr atoms, both at the single-crystal surfaces and in the interior of the grains.

It is worth noticing that Zr is the chemical element which acts as the preferential partner of the absorbed oxygen while Fe and V are found in a metallic configuration in the volume of the grains.[21] Moreover, the Zr-oxide stoichiometry is in agreement with the value of 2.2 found previously for the ratio (number O atoms)/(number of metallic atoms).[21] We remark that x-ray diffraction measurements indicated that interaction of the alloy pills with water promoted a drastic change of the alloy structure towards an amorphous character. However, these measurements could not identify the actual pattern of phases and relative stoichiometries of the water-treated $[Zr(V_{0.5}Fe_{0.5})_2]$ alloy.

Concerning the distinct role of Zr atoms in gettering most of the oxygen-containing groups compared to the metal-like behavior of both Fe and V in the WT alloy, we remark that similar trends were observed at the surface of the $ZrV_{0.63}Fe_{0.13}$ alloy after controlled exposures (up to 1000 L)

to H_2O at 700 K, as reported by Vedel and Schlapbach.[10]

IV. CONCLUSIONS

A systematic study of the gettering properties of the $[Zr(V_{0.5}Fe_{0.5})_2]$ alloy with respect to water molecules in an environment modeling an experimental apparatus for recycling tritiated water has been presented. Pills of the water-treated $[Zr(V_{0.5}Fe_{0.5})_2]$ alloy are found to be strongly oxidized in their interior, with O atoms and (OH)-related groups being primarily bonded to Zr atoms. In contrast, Fe and V atoms are identified in a metal-like configuration in the grain volume even after appreciable water dissociation and absorption.

ACKNOWLEDGMENT

The authors are indebted to SAES Getters S.pA. Company for providing the virgin alloys.

[1]C. Boffito, B. Ferrario, P. della Porta, and L. Rosai, J. Vac. Sci. Technol. **18**, 1117 (1981).
[2]R. J. Knize and L. Cecchi, J. Vac. Sci. Technol. A **1**, 1273 (1983); **1**, 1276 (1983).
[3]W. V. Lampert, K. D. Rachocki, B. C. Lamartine, and T. W. Haas, J. Vac. Sci. Technol. **18**, 1121 (1981).
[4]H. C. Hseuh and C. Lanni, J. Vac. Sci. Technol. A **1**, 1283 (1983).
[5]K. Ichimura, N. Inoue, K. Watanabe, and T. Takeuchi, J. Vac. Sci. Technol. A **2**, 1341 (1984).
[6]K. Ichimura, N. Inoue, K. Ashida, K. Watanabe, and T. Takeuchi, J. Nucl. Mater. **128/129**, 876 (1984).
[7]F. Meli, Z. Sheng, I. Vedel, and L. Schlapbach, Vacuum **41**, 1938 (1990).
[8]K. Ichimura, M. Matsuyama, and K. Watanabe, J. Vac. Sci. Technol. A **5**, 220 (1987).
[9]M. Sancrotti, G. Trezzi, and P. Manini, J. Vac. Sci. Technol. A **9**, 182 (1991).
[10]I. Vedel and L. Schlapbach, J. Vac. Sci. Technol. A **11**, 539 (1993).
[11]J. Kovac, O. Sakho, P. Manini, and M. Sancrotti, Surf. Interface Anal. **22**, 327 (1994).
[12]M. Sancrotti, Proceedings of the 16th IUVSTA Workshop on Outgassing Properties of Materials; The Kinetics and Thermodynamics of Adsorption, Desorption, and Passivation, edited by B. Hjörvarsson and L. Westerberg, Uppsala, Sweden, 1997 (unpublished).
[13]N. Venkataramani, A. Conte, F. Ghezzi, G. Bonizzoni, and C. Boffito, J. Nucl. Mater. **200**, 343 (1993).
[14]F. Ghezzi, A. Conte, N. Ventakaramani, and G. Bonizzoni, Z. Physikalische Chemie **183**, 399 (1994).
[15]F. Ghezzi, N. Ventakaramani, A. L. Caterino, G. Bonizzoni, G. Gervasini, and A. Conte, J. Nucl. Mater. **212–215**, 981 (1994).
[16]C. D. Wagner, W. M. Riggs, L. E. Davies, J. F. Moulder, and G. E. Muilenberg, *Handbook of X-ray Photoelectron Spectroscopy* (Perkin–Elmer, Eden Praire, MN, 1979); J. F. Moulder *et al.*, *Handbook of X-ray Photoelectron Spectroscopy*, edited by J. Chastain (Perkin–Elmer Corp., Eden Prairie, MN, 1992).
[17]C. Morant, J. M. Sanz, L. Galan, L. Soriano, and F. Rueda, Surf. Sci. **218**, 331 (1989).
[18]R. Kaufmann, H. Klewe-Nebenius, H. Moers, G. Pfennig, H. Jenett, and H. J. Ache, Surf. Interface Anal. **11**, 502 (1988).
[19]*Sputtering by Particle Bombardment*, edited by R. Behrisch (Springer, Berlin, 1983), Vol. II.
[20]See M. Gupta and L. Schlapbach, in *Hydrogen in Intermetallic Compounds*, edited by L. Schlapbach (Springer, Berlin, 1992), Vol. I, Chap. 5.
[21]F. Ghezzi, N. Venkataramani, M. Colombo, A. Conte, G. Bonizzoni, and W. Schmayda, Fusion Technol. **27**, 458 (1995); F. Ghezzi, N. Venkataramani, M. Colombo, G. Bonizzoni, and W. Schmayda, Fusion Technol. **29**, 91 (1996).
[22]While the BE of the Zr 3*d* core level is quite sensitive to the oxidation state of the Zr atoms, the O 1*s* core line emission is found to be much less sensitive to the oxide stoichiometry.